Available online at www.sciencedirect.com

SciVerse ScienceDirect

Physics Procedia 36 (2012) 144 – 149

Physics Procedia

Superconductivity Centennial Conference

Integrated directly-coupled SQUID magnetometer and gradiometer

Chan-Yao Chang, Chi-Ming Hsu, and Jen-Tzong Jeng[a]*

[a]*Institute of Mechanical and Precision Engineering, National Kaohsiung University of Applied Sciences, Kaohsiung 80778, Taiwan, ROC.*

Abstract

In this work, we investigated the directly-coupled superconducting quantum interference device (SQUID) magnetometer and gradiometer with integrated pickup loops. To prepare the structures, we fabricated the $YBa_2Cu_3O_{7-x}$ thin films on strontium titanate ($SrTiO_3$) substrates by magnetron rf sputtering. The devices were patterned by ultra-violet photolithography followed by a three-step wet etching process. The circular and differential modulation coils for the magnetometer and gradiometer, respectively, were wound on bakelite frames attached to the back of the chip mount. The voltage-current and voltage-flux characteristics of option SQUIDs on the chip, which was put in a switching-channel electrical cryostat, were characterized by using the low-noise preamplifier, the homemade current-waveform generator, and the computer-based data acquisition unit. The magnetometer and the gradiometer can be operated simultaneously by independent flux-locked loops. The proposed sensor can be applied to the nondestructive evaluation and biomagnetic imaging, for example, magnetocardiogram.

Keyword: SQUID; magnetometer; gradiometer;

1. Introduction

The superconducting quantum interference device (SQUID) is known for its ultra-high sensitivity in sensing weak magnetic fields [1]. To achieve a high sensitivity for unshielded operation, the design of a dc SQUID gradiometer typically comprises a large differential pickup coil inductively coupled to the small loop of two grain-boundary Josephson junctions in parallel [2]. Although the coupling efficient is

* Corresponding author.
E-mail address: jeng.jt@gmail.com.

1875-3892 doi:10.1016/j.phpro.2012.06.061

relatively low, the directly-coupled design implemented with single-layered superconducting film can achieve low noise because the high-quality crystalline film avoids the noise arising from flux trapping. However, e.g. when the sensor rotates in Earth's magnetic field, large circumferential shielding currents can drive the magnetic flux to penetrate the superconducting film of differential pickup coil and induce excess low frequency noise. In order to solve circumferential shielding currents, V Schultze *et al.* [3] reported a design consisting of directly coupled gradiometer and magnetometers on the same chip. The gradiometer is used to measure magnetic field gradient while the flux-locked magnetometer keeps the magnetic field in gradiometer's pickup coil virtually zero. Namely, a magnetometer can not only measure the magnetic field but also provide a feedback to null the field in gradiometer. Recently, Steppke *et al.* [4] presented an integrated planar gradiometer having orthogonal pickup coils on a $SrTiO_3$ substrate containing two grain boundaries. This device can simultaneously measure the magnetic field gradients along two directions. Nevertheless, as circumferential shielding currents also occur in the antenna structure, it is important to overcome the noise due to magnetic fields in unshielded environment in order to reach a highly stable operation. In this paper, we study the fully integrated directly-coupled SQUID magnetometer and gradiometer with shared pickup loops. By using circular and differential modulation coils, the magnetometer and the gradiometer can be operated simultaneously by using independent flux-locked loops. The characteristics of the device implemented on a bicrystal substrate were discussed.

2. Experimental details

2.1. Design of integrated gradiometer and magnetometer

Here we proposed a novel directly-coupled SQUID magnetometer and gradiometer with integrated pickup loops, as shown in Fig. 1. The pickup coil of gradiometer are also shared by the magnetometer. In this way, the effective areas of both gradiometer and magnetometer are maximized in limited area of the same chip. To avoid the magnetometer's response to gradient signal, the bicrystal line is aligned along the strip's center of one branch in the SQUID body of magnetometer. In this way, the induced current from differential pickup loop carrying the gradient signal does not generate magnetic flux in the SQUID loop of magnetometer. In addition, the gradiometer channel does not response to the magnetometer signal since the SQUID loop of gradiometer detects only the induced current from differential pickup loop.

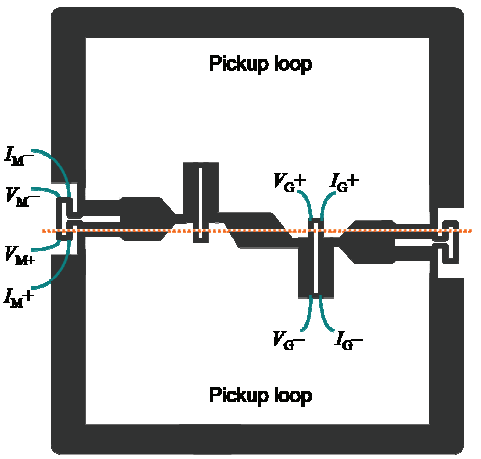

Fig. 1 Design of the integrated SQUID magnetometer and gradiometer.

2.2. Effective areas

For a directly-coupled SQUID magnetometer with bicrystal Josephson junctions [2], the effective area is determined by its geometrical parameters. Provided that the magnetic field, Bin, is normal to the plane of pickup coil, the induced superconducting shielding current is $I_p = B_z A_p / L_p$, where A_P is the pickup area and L_P is the inductance of pickup loop. The magnetic flux in the SQUID body induced by I_p injecting to the SQUID loop is $\Phi_i = L_i I_p = \alpha L_S I_p$, in which L_i is the injection inductance, L_S is the inductance of SQUID body, and α is a dimensionless coupling coefficient defined as $\alpha = L_i / L_S$. The SQUID inductance, L_S, is the inductance seen by the circulation current around the SQUID hole. It follows the relation $L_S = L_i + L_j$, where L_j is the inductance of the loop connecting the two junctions. Given A_S be the area of SQUID body, the magnetic flux threading the SQUID body due to B_z is $\Phi_{th} = B_z A_S$, and the total magnetic flux in the SQUID is: $\Phi_S = \Phi_i + \Phi_{th}$. Therefore, the effective area of a directly-coupled magnetometer, which is defined as the total magnetic flux, Φ_S, in SQUID body divided by the applied magnetic field, B_z, is [2]:

$$A_{eff} = \alpha \frac{L_S A_p}{L_p} + A_S \tag{1}$$

The last term can be neglected when the effective area is much greater than the parasitic area of SQUID body. For our magnetometer design made from a 140 nm film, the area of pickup loop is $A_p \approx 50$ mm^2 and the inductance is $L_p \approx 20$ nH. The inner lengths of the "T-shaped" SQUID hole are 30μm for vertical and 71 μm for horizontal. The parasitic area is calculated to be $A_S = 1.3\times10^{-3}$ mm^2, and the estimated inductance is $L_S \approx 100$ pH [5]. The coupling coefficient determined by mutual-inductance calculation is $\alpha \approx 0.6$, and the effective area calculated by (1) is found to be $A_{eff} \approx 0.15$ mm^2.

For a first-order directly-coupled SQUID gradiometer, the current induced in the differential pickup loop, I_p, is the response to the first order gradient of B_z along its baseline direction. Given the baseline length ℓ, the difference in magnetic field between the two branch of differential pickup loops is $\Delta B = \ell (dB_z / dx)$, where x is the coordinate along the baseline. The argument similar to those for (1) can be applied to derive the effective area of gradiometer. The effective area of a directly-coupled gradiometer is defined as the total magnetic flux, Φ_S, in SQUID body divided by ΔB. The obtained effective area is similar to (1) with A_S neglected:

$$A_{eff,g} = \alpha_g \frac{L_{S,g} A_{p,g}}{L_{p,g}} \tag{2}$$

where $A_{p,g}$ and $L_{p,g}$ denotes area and inductance for each branch of differential pickup loop, and $L_{S,g}$ is the SQUID inductance of gradiometer. For our design, $A_{P,g} = 0.5A_P \approx 25$ mm^2 and $L_{P,g} = 0.5L_P \approx 20$ nH. The SQUID hole of gradiometer is 70 μm in length and the SQUID area is calculated to be 0.8×10^{-3} mm^2. The estimated SQUID inductance is $L_S \approx 70$ pH [5], the coupling coefficient is $\alpha_g \approx 0.7$, and the effective area for the gradiometer calculated by (2) is found to be $A_{eff} \approx 0.12$ mm^2.

2.3. Modulation schemes

The circular and differential modulation coils for the magnetometer and gradiometer, respectively, were wound on bakelite frames. Fig. 2(a) shows how can the modulation coils drive the magnetometer and gradiometer simultaneously with minimum crosstalk. The spatial distribution of gradient modulation field in the device is shown in Fig. 2(b). As the gradient modulation field generates zero net magnetic flux in the magnetometer pickup loop, it does not induce a magnetic signal in the magnetometer SQUID if the modulation coils were aligned exactly on the symmetric axes.

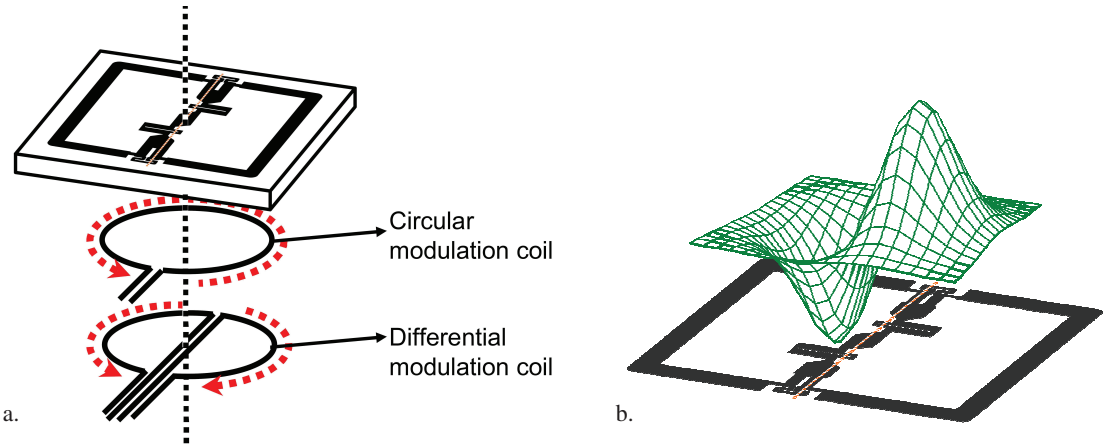

Fig. 2 Modulation scheme of the integrated magnetometers and gradiometers: (a) Arrangement of one circular and one differential modulation coil for magnetometer and gradiometer; (b) Spatial distribution of modulation field in the device.

2.4. Device fabrication

The device was made from a crystalline superconducting film grown on a 10 mm × 10 mm $SrTiO_3$ 24º/24º bicrystal substrate. To preparation the high-T_c superconducting thin films with highest T_c around 90 K, we worked hard to find the optimum deposition conditions. A 140-nm thick $YBa_2Cu_3O_{7-x}$ film was deposited by high-pressure magnetron rf sputtering in a 0.39-torr atmosphere of oxygen and argon, for which the flow rates are 95 and 42 sccm. respectively. The substrate temperature were found to be around 800ºC with the heater's power output at 58.7 %. After deposition, the film were annealed in-situ in an 540 torr oxygen atmosphere with the heater's power output at 32.3 %. To reduce the contact resistance of device, a silver film of about 100 nm in thickness was deposited by magnetron DC sputtering with a shadow mask covering the region along bicrystal line. The pattern of device were then patterned with ultra-violet photolithography followed by a three-step wet etching process. The microscopic photograph of the SQUIDs in the device were shown in Fig. 3(a). To avoid over etching, the 3-μm micro-bridges in the pattern were repeatedly checked with an optical microscope during the etching process. After wire bonding the device with chip mount, the sample is put in a switching-channel cryostat to characterize the voltage-current (*V-I*) and voltage-flux (*V-B*) curves as shown in Fig. 3(b). The cryostat were cooled to the temperature of 77 K by immersing it in liquid nitrogen in an open Dewar flask. The temperature was further reduced to T = 63 K by pumping on the liquid nitrogen bath when necessary. Several option SQUIDs on the chip were biased with a homemade current-waveform generator, and their voltage outputs were detected by using a low-noise preamplifier (MODEL SR560 from Stanford Research Systems) with a total gain between 103 to 104. The *V-I* and *V-B* wave forms were captured by using a computer-based data acquisition unit (NI DAQ6008) controlled by a program coded in our laboratory.

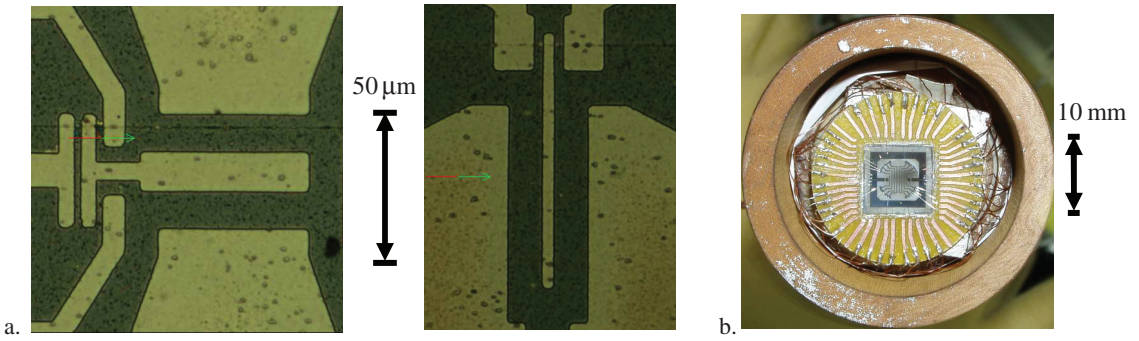

Fig. 3(a) Optical micrographs of SQUID for magnetometer (left) and gradiometer (right) at the magnification of 500x. The junction width is 3 μm. (b) Photograph of the integrated magnetometer and gradiometers mounted on the cryostat.

3. Results and Discussion

The voltage-current characteristics of SQUIDs for magnetometer and gradiometer at 63 K are shown in Fig. 4. We estimated the total critical current to be I_c = 1 mA, and the normal resistance R_n = 0.1 Ω for magnetometer. For the gradiometer, the critical current is I_c = 0.55 mA and the normal resistance R_n = 2 Ω. , By fitting the measured voltage-current characteristics to an RSJ model [6] with excess current [7], the excess currents were both found to be 0.3 mA, corresponding to 30% and 60% respectively for the SQUIDs of magnetometer and gradiometer. The large excess current should be due to superconducting micro-shorts across the grain boundary. By considering the excess current, the effective characteristics voltage are 74 μV and 400 μV respectively for the junctions in the SQUIDs of magnetometer and gradiometer. It shows a large critical current.

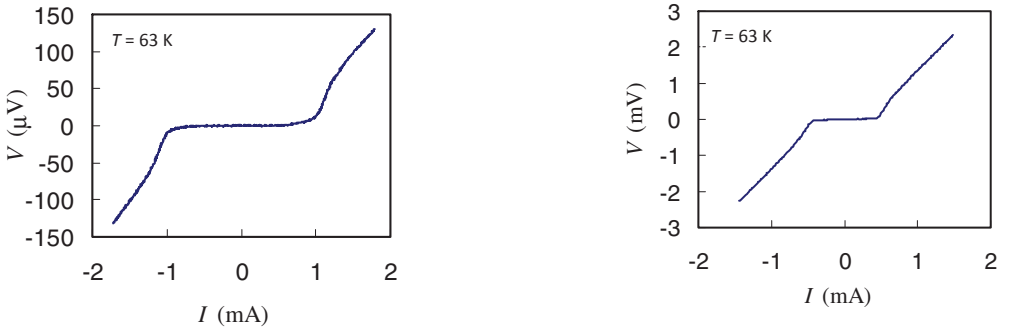

Figure. 4 The *V-I* curve of SQUID for magnetometer (left) and gradiometer (right).

The voltage-field characteristics of the SQUID of magnetometer at 63 K is shown in Fig. 5. The maximum negative voltage swing was 30 μV. However, it was found that the curves are generally non-periodic, which may be due to the grain boundaries crossing the pickup loop acting as flux dams. The field-to-voltage transfer coefficient were found to be dV/dB = 1.2 V/T. The relatively small dV/dB is due to the small normal resistance of R_n = 0.1 Ω arising from the spreads in critical current and normal resistance of junctions. Further works to make the device with more options SQUID on a chip is the practical way to optimize its voltage-flux characteristics. Improving the characteristics of junctions is crucial to realized a high-Tc SQUID integrated magnetometer and gradiometer with high performance.

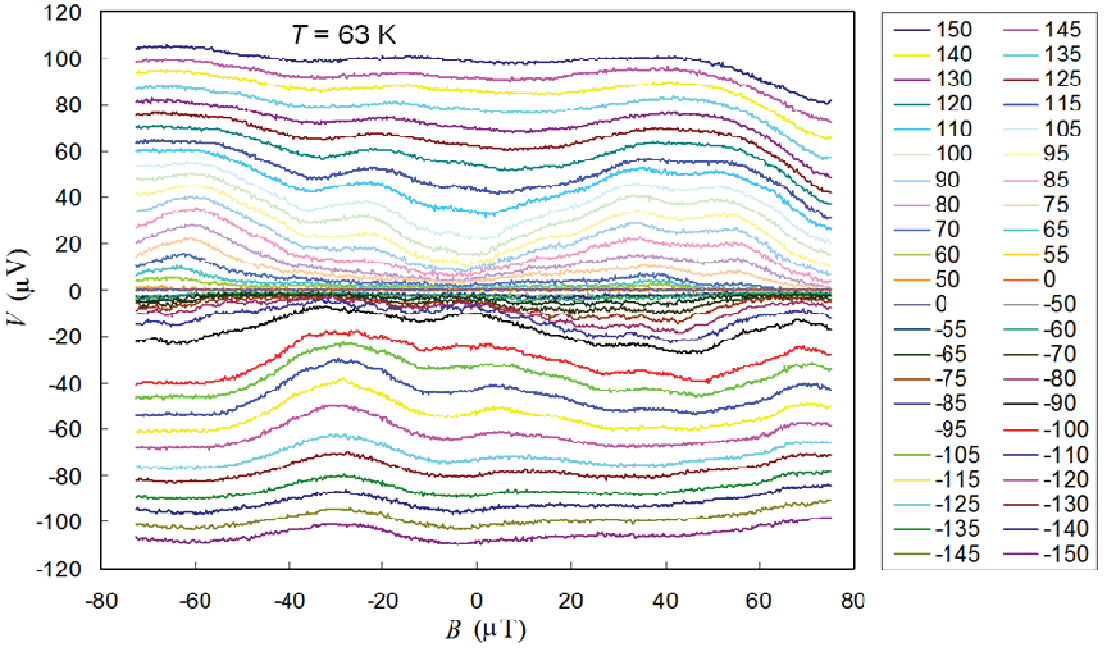

Figure. 5 The V-B curve of SQUID for magnetometer.

Acknowledgements

This work is supported by the National Science Council of Taiwan under Grant No. NSC98-2112-M-151-002-MY3.

References

[1] J. Clarke, A. I. Braginski, *The SQUID Handbook: Vol. I Fundamentals and Technology of SQUIDs and SQUID Systems*, Wiley VCH; 2004.

[2] D. Koelle, R. Kleiner, F. Ludwig, E. Dantsker and John Clarke, High-transition-temperature superconducting quantum interference devices, Reviews of Modern Physics 71; 1999, p.631.

[3] Volkmar Schultze, Rob IJsselsteijn, Torsten May, and Hans-Georg Meyer, Highly balanced single-layer high-temperature superconductor SQUID gradiometer freely movable within the Earth's magnetic field, Institute of Physics Supercond. Sci. Technol., vol. 16; 2003, p. 773-777.

[4] A. Steppke, C. Becker, V. Grosse, L. Dörrer, F. Schmidl, P. Seidel, M. Djupmyr, and J. Albrecht, Planar high-T_c superconducting quantum interference device gradiometer for simultaneous measurements of two magnetic field gradients, Appl. Phys. Lett., vol. 92, article no. 122504; 2008.

[5] Frederick W. Grover, Inductance calculation: working formulas and tables, New York: Nostrand; 1947.

[6] J.T. Jeng, H.C. Hung, C.R. Lin, C.H. Wu, K.L. Chen, J.C. Chen, H.C. Yang, S.H. Liao, and H.E. Horng, Flux-to-voltage transfer function of the series-SQUID array with grain-boundary Josephson junctions, IEEE Trans. Appl. Supercond., vol. 15; 2005, p. 793-796.

[7] R. G. Seed and C. Vittoria, Excess current in shunted Josephson weak links, J. Appl. Phys. 75; 1994, p. 8195-8197.